Available online at www.sciencedirect.com
ScienceDirect
Nuclear Medicine and Biology 34 (2007) 1003–1008
NUCLEAR MEDICINE — AND — BIOLOGY
www.elsevier.com/locate/nucmedbio

Pharmacokinetics of 3-[^{125}I]iodo-α-methyl-L-tyrosine, a tumor imaging agent, after probenecid loading in mice implanted with colon cancer DLD-1 cells

Syuichi Nakajima[a,b], Naoto Shikano[a,*], Takashi Kotani[a], Masato Ogura[a], Ryuichi Nishii[c], Mitsuyoshi Yoshimoto[b], Naoto Yamaguchi[d], Yukio Iwamura[e], Nobuo Kubota[a], Nobuyoshi Ishikawa[a], Keiichi Kawai[b]

[a]*Department of Radiological Sciences, Ibaraki Prefectural University of Health Sciences, 4669-2 Ami, Ami-machi, Inashiki-gun, Ibaraki 300-0394, Japan*
[b]*Division of Health Science, Graduate School of Health Sciences, Kanazawa University, 5-11-80 Kodatsuno, Kanazawa, Ishikawa 9200-942, Japan*
[c]*Research Institute, Shiga Medical Center, 5-4-30 Moriyama, Moriyama-City, Shiga 524-8524, Japan*
[d]*Center for Medical Sciences, Ibaraki Prefectural University of Health Sciences, 4669-2 Ami, Ami-machi, Inashiki-gun, Ibaraki 300-0394, Japan*
[e]*Center for Humanities and Sciences, Ibaraki Prefectural University of Health Sciences, 4669-2 Ami, Ami-machi, Inashiki-gun, Ibaraki 300-0394, Japan*

Received 25 June 2007; accepted 28 June 2007

Abstract

Introduction: In order to improve tumor imaging, changes in the pharmacokinetics of 3-[^{123}I]iodo-α-methyl-L-tyrosine ([^{123}I]IMT), an artificial amino acid that exhibits high tumor accumulation, after probenecid (PBC) loading was studied in mice implanted with colon cancer DLD-1 cells using ^{125}I-labeled IMT ([^{125}I]IMT).
Methods: DLD-1-implanted KSN-slc nude male mice received 740 kBq of [^{125}I]IMT via the tail vein at 5 min after 50 mg/kg body weight PBC loading, and autoradiography was performed at 5, 15 and 30 min after injection. Male ddY mice then received 670 kBq of [^{125}I]IMT and 50 mg/kg 2-amino-bicyclo[2,2,1]heptane-2-carboxylic acid (BCH) or *p*-aminohippurate (PAH) via the tail vein, and kidney autoradiography was performed at 5 min after injection. In vitro inhibition study was then performed based on the accumulation mechanisms of [^{125}I]IMT in DLD-1, using 1 mM L-tyrosine, BCH, α-(methylamino)-isobutyric acid, *N*-benzoyl-β-alanine, PBC, PAH, 2,4-dinitrophenol and sodium azide. Both Na^+-dependent and Na^+-independent uptake were investigated.
Results: Higher tumor accumulation in PBC-loaded DLD-1-implanted mice was seen when compared to control mice. PAH and BCH, respectively, reduced renal accumulation in the tubule segment-2 (S2)-like and S1-like regions. We confirmed that [^{125}I]IMT transport is predominantly mediated by L-type amino acid transporter-1 in DLD-1 cells.
Conclusions: [^{125}I]IMT uptake is mediated by organic anion and amino acid transporters in the kidney. Organic anion transporter inhibitors may yield better tumor images with good tumor/normal tissue radioactivity ratios if adequate administration plans are developed.

Keywords: Abdominal tumor imaging; Amino acid transport; Colon cancer cell line; DLD-1; 3-Iodo-α-methyl-L-tyrosine; Organic anion transport inhibitor

1. Introduction

The search for strategies to improve amino acid imaging may facilitate further research into oncology tracers. Since the 1970s, the artificial amino acid 3-[^{123}I]iodo-α-methyl-L-tyrosine ([^{123}I]IMT) has been successfully used in single-photon emission computed tomography (SPECT) imaging of brain tumors [1–4]. Recent studies indicate that ^{125}I-labeled IMT ([^{125}I]IMT), a substrate of L-type amino acid transporter-1 (LAT1; component of amino acid transport system L) [5], is one of the most promising radiopharmaceuticals for use as a tumor imaging agent in SPECT, because LAT1 is expressed in numerous tumor tissues at higher levels than in normal tissues [6]. However, relatively few studies have investigated extracranial tumors with [^{123}I]IMT, as high physiological [^{123}I]IMT accumulation is

* Corresponding author. Tel.: +81 29 840 2217; fax: +81 29 840 2317.
E-mail address: sikano@ipu.ac.jp (N. Shikano).

0969-8051/$ – see front matter © 2007 Elsevier Inc. All rights reserved.
doi:10.1016/j.nucmedbio.2007.06.017

observed in the kidney, and this has been an obstacle for abdominal tumor imaging with good tumor/normal tissue radioactivity ratios. Several α-methylated tyrosine analogues, such as [^{123}I]IMT and 3-[^{18}F]fluoro-α-methyl-L-tyrosine ([^{18}F]FMT), also exhibit high accumulation in the renal cortex [7]. We recently proposed that α-methylated tyrosine analogues possess a higher affinity for accumulative renal organic anion secretion systems than non-α-methylated tyrosine analogues [8]. Thus, we hoped that organic anion transporter (OAT) inhibitors could improve abdominal tumor imaging via inhibition of accumulative secretion of [^{125}I]IMT in proximal tubules, as OATs are thought to mediate the accumulative renal elimination of [^{125}I]IMT via proximal tubule segment-2 (S2) [9,10].

Using in vivo autoradiography, we studied the changes in [^{125}I]IMT pharmacokinetics by administration of probenecid (PBC, an organic anion secretion inhibitor in the kidney) [11] in DLD-1 (colon cancer cell line)-implanted male nude mice (KSN-slc). To clarify the renal transport of [^{125}I]IMT, renal autoradiography of normal male ddY mice treated with specific system L inhibitors or specific OAT inhibitors was conducted. Furthermore, in vitro inhibition tests into the accumulation mechanisms of [^{125}I]IMT in DLD-1 were conducted in order to confirm the roles of amino acid transporter(s).

Based on the results of in vivo whole-body autoradiography in DLD-1-implanted mice administered [^{125}I]IMT with PBC loading, we also discuss the effects of PBC loading on target tumor tissue (DLD-1) and nontarget organs (particularly the kidney).

2. Materials and methods

Animal experiments were approved by the ethics committee of Ibaraki Prefectural University of Health Sciences. We used longer lived [^{125}I]IMT rather than [^{123}I]IMT for convenience in this experiment.

2.1. Materials and preparation of [^{125}I]IMT

L-Tyrosine (mother compound of [^{123}I]IMT), 2-aminobicyclo[2,2,1]heptane-2-carboxylic acid (BCH, specific system L inhibitor) [12], α-(methylamino)-isobutyric acid (MeAIB, specific system A inhibitor) [13], *N*-benzoyl-β-alanine (BBA, OAT inhibitor) [14], PBC, *p*-aminohippurate (PAH, specific OAT inhibitor) [15], 2,4-dinitrophenol (DNP, inhibitor of anaerobic mitochondrial energy production) [16, 17], sodium azide (NaN_3, inhibitor of aerobic energy production) [17], α-methyl-L-tyrosine and chloramine-T were acquired from Sigma-Aldrich Japan K.K. (Tokyo, Japan). [^{125}I]NaI (629 GBq/mg) was obtained from American Radiolabeled Chemicals Inc. (St. Louis, MO, USA). Nova-Pak C-18 (3.9×300 mm; Waters, Milford, MA, USA) was used for separation and rectification. For cell line studies, the human colorectal adenocarcinoma cell line DLD-1 was obtained from the Japanese Collection of Research Bioresources (Tokyo, Japan; catalog number JCRB9094). Plastic tissue culture dishes (diameter, 60 mm; Nalge Nunc International, Roskilde, Denmark) and plastic flasks (surface area, 25 cm^2; Nalge Nunc International) were used. No-carrier-added [^{125}I]IMT was prepared using the conventional chloramine-T method, as described elsewhere [5].

2.2. Cell cultures

DLD-1 cells were maintained in Dulbecco's modified Eagle's medium (Sigma-Aldrich Japan) supplemented with L-glutamine (2 mM) and 10% fetal bovine serum without antibiotics, in an atmosphere of 10% CO_2 and 90% air at 37°C (pH 7.4). Subculturing was performed every 4 days using 0.02% EDTA and 0.05% trypsin. Approximately 5×10^5 cells per dish were replanted in plastic tissue culture dishes (diameter, 60 mm; Nalge Nunc International) 4 days after experimental use.

2.3. In vivo whole-body autoradiography in DLD-1-implanted mice administered [^{125}I]IMT with PBC loading

At 7 to 10 days after implantation of 3×10^6 cells per mouse, DLD-1-implanted male KSN-slc mice (n=6; weight, 20 g; age, 6 weeks) received 0.1 ml of [^{125}I]IMT (740 kBq) and 50 mg/kg of PBC by injection into the tail vein 5 min prior to [^{125}I]IMT injection. Mice were sacrificed by inspiration of excess ether at 5, 15 and 30 min after [^{125}I]IMT injection, placed in carboxymethyl cellulose embedding medium (Nacalai, Kyoto, Japan) and frozen at −15°C for at least 12 h.

An Autocryotome CM3050 S (Leica, Tokyo, Japan) was used to cut 20-μm sagittal sections. Sections were then dried at −5°C for a further 24 h. Tissue slices were kept in contact with BAS-SR2040 imaging plates (Fuji Photo Film, Kanagawa, Japan) for 6 h. Images were processed using a BAS 2500 Bio-Imaging Analyzer (Fuji Photo Film) [9].

2.4. In vivo renal autoradiography in normal mice with BCH or PAH loading

For renal autoradiography, 0.1 ml of [^{125}I]IMT (670 kBq) was injected into the tail veins of normal male ddY mice (n=3, weight, 25 g) administered 20 mg/kg body weight BCH (simultaneous injection with [^{125}I]IMT) or PAH (5 min prior to [^{125}I]IMT injection) as an inhibitor. Five minutes after [^{125}I]IMT injection, mice were sacrificed by inspiration of excess ether. Kidneys were placed in carboxymethyl cellulose embedding medium (Nacalai) and frozen at −15°C for at least 12 h [8].

2.5. In vitro inhibition study with DLD-1 cells

For the time course study, after removal from culture medium, cells were preincubated with 2 ml of incubation medium for 10 min at 37°C, after which 2 ml of incubation medium containing [^{125}I]IMT (18.5 kBq) was added. Cells were then incubated for a specified period (5, 10, 15 or

30 min) at 37°C. Uptake medium was removed by suction at the end of the incubation period, and cells were rapidly washed twice with 2 ml of ice-cold incubation medium. Cells on the dishes were solubilized in 1.0 ml of 1 N NaOH, and the radioactivity of each aliquot (100 μl) was counted using an auto well counter (Aloka, Japan; ARC-380). Based on the results of this time course study, 10 min was used for uptake incubation in subsequent experiments.

Inhibition experiments were performed in sodium-containing uptake medium (NaCl, 137 mM; KCl, 3.7 mM; Na_2HPO_4, 8.0 mM; KH_2PO_4, 1.5 mM; $CaCl_2 \cdot 2H_2O$, 1.8 mM; $MgCl \cdot 6H_2O$, 1 mM) and sodium-free uptake medium. In the sodium-free experiment, NaCl and Na_2HPO_4 were replaced with the same concentrations of choline chloride and K_2HPO_4. After 10-min preincubation in sodium-containing medium or sodium-free medium, cells were incubated for 10 min with uptake medium containing [^{125}I]IMT (18.5 kBq) with inhibitor in the same manner as in the time course study. The following inhibitors were used at a concentration of 1 mM in order to examine inhibition of [^{125}I]IMT uptake; L-tyrosine, BCH, MeAIB, BBA, PBC, PAH, DNP and NaN_3.

2.6. Statistical analysis

Values obtained in each experiment are expressed as means±S.D. Statistical comparisons between groups were performed using Student's *t* test.

3. Results

3.1. In vivo whole-body autoradiography in DLD-1-implanted mice administered [^{125}I]IMT with PBC loading

Fig. 1A and B, respectively, shows a typical whole-body autoradiograph and relative [^{125}I]IMT accumulation in organs and implanted tumors. The highest radioactivity was seen in the kidneys, followed by the pancreas and implanted tumor, in all mice. Tumor radioactivity ratios with

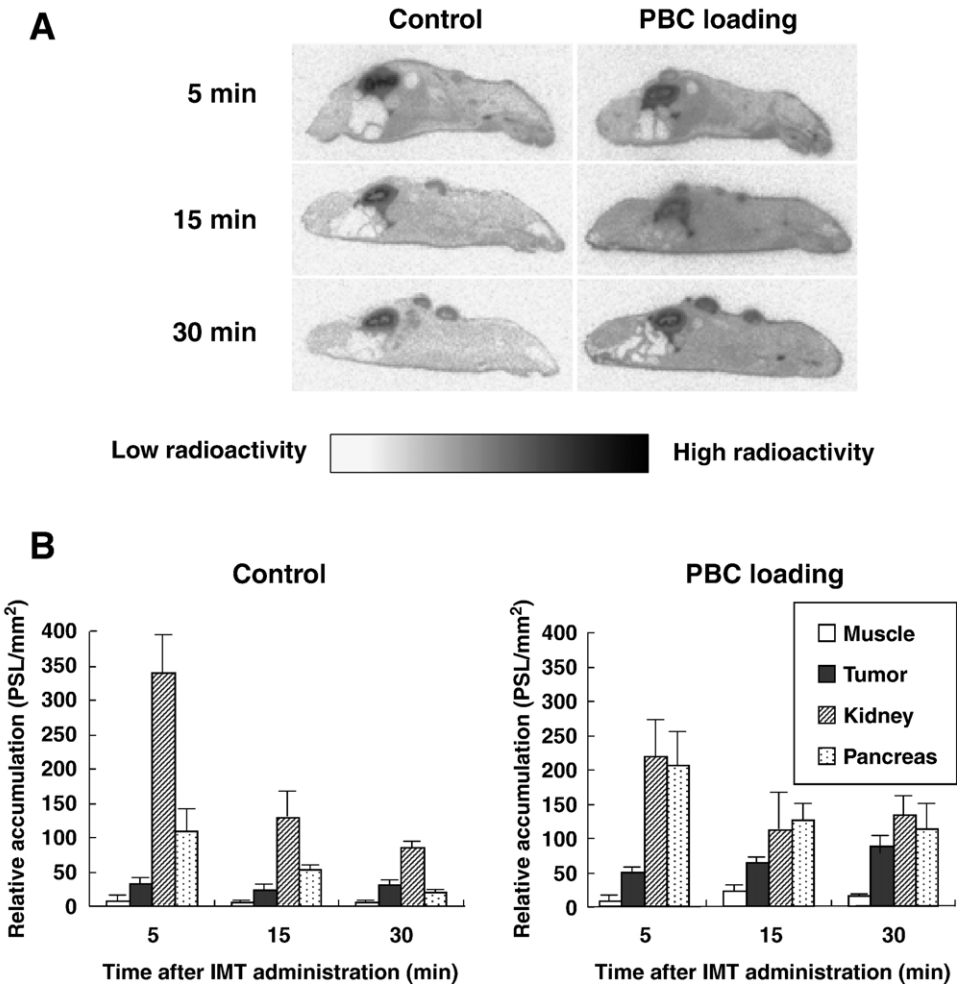

Fig. 1. Whole-body autoradiograph of DLD-1 (colon cancer cell line)-bearing KSN-slc male mice (left, without PBC loading, control; right, with PBC loading) (A). Relative accumulation in organs and implanted DLD-1 (B) at 5, 15, and 30 min after [^{125}I]IMT administration. DLD-1 cells were implanted under the back skin of mice. The tumor/muscle ratios were about 5 for control mice and about 7 for PBC-loaded mice at 30 min after [^{125}I]IMT injection. Photostimulated luminescence (PSL) intensity of luminescence radiation when the imaging plate was scanned with the laser in a Fuji bioimaging analyzer. PSL per millimeter squared is proportional to becquerels per millimeter squared. The highest radioactivity was seen in the kidney, followed by the pancreas and implanted tumor.

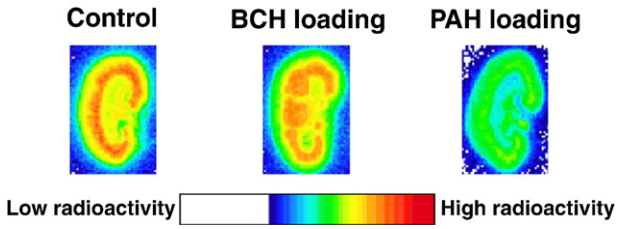

Fig. 2. Renal autoradiograph of normal male ddY mice administered BCH or PAH at 5 min after [^{125}I]IMT administration. BCH inhibits systems L, B^0 and B^{0+} in the presence of sodium. PAH is an inhibitor of OATs.

PBC loading were 1.5-fold higher at 5 min and 2.8-fold higher at 15 and 30 min when compared to control mice. The tumor/muscle ratios were approximately 5 for control mice and 6 to 7 for PBC-loaded mice at 30 min after [^{125}I]IMT injection.

3.2. In vivo renal autoradiography in normal mice with BCH or PAH loading

[^{125}I]IMT accumulated mainly in the renal cortex, but this was reduced by BCH loading in the S1-like region and by PAH loading in the S2-like region of proximal tubule segments (Fig. 2).

3.2.1. In vitro inhibition study with DLD-1 cells

Time course analysis of [^{125}I]IMT uptake into DLD-1 cells revealed that steady-state levels were reached 10 min after the start of incubation, as shown in Fig. 3. Thus, a 10-min incubation time was used for the inhibition study.

The results of the [^{125}I]IMT uptake inhibition experiments are shown in Fig. 4. L-Tyrosine (mother compound of [^{123}I]IMT) and BCH (specific system L inhibitor) significantly inhibited [^{125}I]IMT uptake (P<.01). BBA (OAT inhibitor), PBC (OAT inhibitor), PAH (OAT specific inhibitor), DNP (inhibitor of anaerobic mitochondrial energy production) and NaN_3 (inhibitor of aerobic energy production) had little inhibitory effect on [^{125}I]IMT uptake. Replacing sodium with choline reduced [^{125}I]IMT transport into DLD-1 cells, but the effect was not significant.

Transport of [^{125}I]IMT into DLD-1 cells was predominantly (71%) mediated by a Na^+-independent system, with a minor contribution from a Na^+-dependent system (Fig. 5). At 1 mM, the amino acids BCH (with and without sodium) and L-tyrosine inhibited accumulation of [^{125}I]IMT to similar degrees (P<.001). This suggests that system A and ASC or another Na^+-dependent system(s) may contribute to Na^+-dependent [^{125}I]IMT transport. MeAIB (specific system A inhibitor) also exhibited an inhibitory effect, but it was not significant.

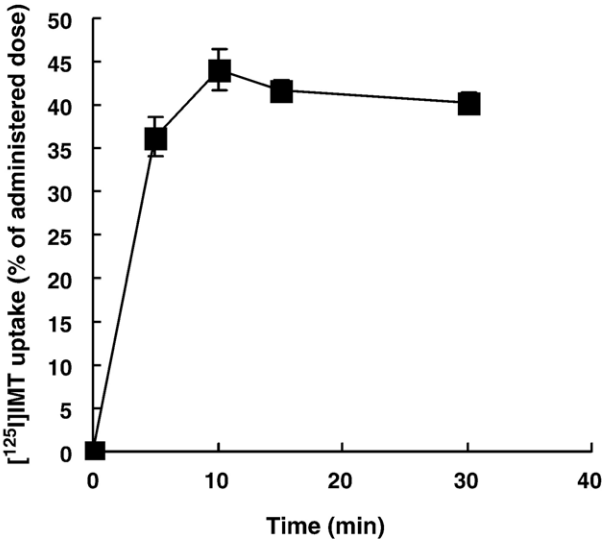

Fig. 3. Time course of [^{125}I]IMT uptake into DLD-1 cells.

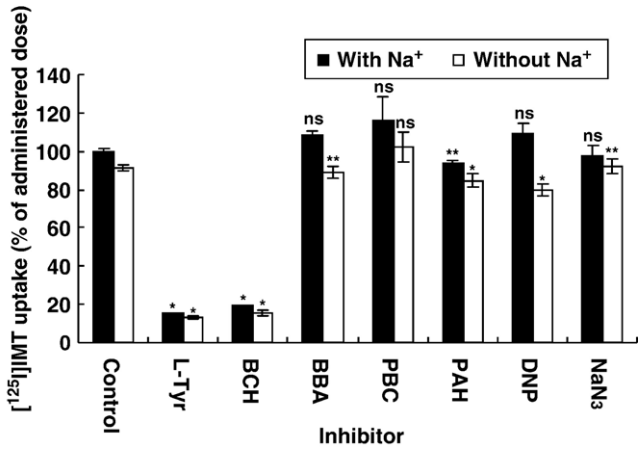

Fig. 4. Effects of inhibitors (1 mM) on uptake of [^{125}I]IMT. Each column represents the mean±S.D. of five plates of DLD-1 cells. *P<.001 vs. control; **P<.01 vs. control; ns, not significant vs. control.

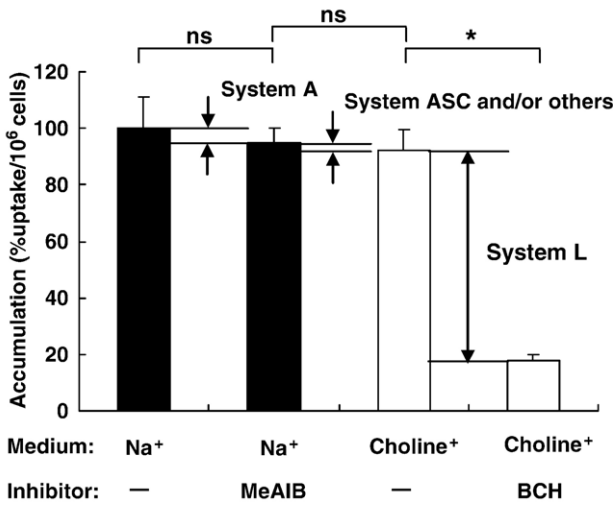

Fig. 5. Experimental determination of neutral amino acid transport systems involved in [^{125}I]IMT accumulation in DLD-1 cells. Each column represents the mean±S.D. of five plates of DLD-1 cells. *P<.001 vs. control; ns, not significant vs. control.

4. Discussion

[^{123}I]IMT was first synthesized in the 1970s by Biersack et al. [1]. It is a nonmetabolizable artificial amino acid that has been used clinically for SPECT imaging of tumors by Kuwert et al. [2], Jager et al. [3] and Langen et al. [4,18]. [^{123}I]IMT exhibits high tumor accumulation and rapid renal elimination [19].

It is known that renal physiological accumulation of [^{125}I]IMT is higher than that of radiolabeled L-tyrosine, its mother compound [4]. We have also observed marked renal accumulation and rapid urinary excretion of [^{125}I]IMT in mice [9]. As shown in Fig. 2, [^{125}I]IMT accumulation was primarily seen in the renal cortex. Clarification of these accumulation mechanisms could aid in developing methods to reduce physiological accumulation, which obstructs abdominal tumor imaging [9].

The kidney is an important nontarget organ for improving obtained images. We examined [^{125}I]IMT distribution in the kidney by in vivo renal autoradiography in normal mice with PAH loading. The reduced [^{125}I]IMT accumulation by PAH loading in the S2-distributed region (inner side of the kidney cortex) suggests that [^{125}I]IMT is transported by OAT(s). Other substrates of OATs (furosemide and ethacrynic acid) also inhibited the tubular secretion and kidney accumulation of [^{125}I]IMT in mice [9].

We therefore tested whether OAT inhibitors (e.g., PAH, PBC and BBA) could improve abdominal tumor images by inhibiting accumulative secretion or [^{125}I]IMT in proximal tubules, as OATs are thought to mediate the accumulative renal elimination of [^{123}I]IMT via proximal S2. The whole-body autoradiographs and relative [^{125}I]IMT accumulation in some organs confirmed that PBC effectively inhibited renal [^{125}I]IMT elimination. The radioactivity ratio of the tumor with PBC loading was approximately threefold higher at 15 and 30 min when compared to control mice. The tumor/muscle ratios were approximately 5 for control mice and 6 to 7 for PBC-loaded mice at 30 min after [^{125}I]IMT injection.

The present results suggest that organic anion inhibitors can effectively reduce kidney accumulation without inhibiting [^{125}I]IMT uptake into target DLD-1 cells provided that an adequate administration plan is developed. In the target tumor cells (DLD-1), there was little or no significant inhibition of [^{125}I]IMT uptake with PAH, PBC or BBA (organic anion inhibitors) loading, while BCH and L-tyrosine (amino acid system L inhibitors) significantly inhibited [^{125}I]IMT uptake. DNP and NaN_3 (inhibitor of energy production) had no significant inhibitory effect on [^{125}I]IMT uptake. Transport of [^{125}I]IMT into DLD-1 cells was largely mediated by an energy- and Na^+-independent transport system (system L), with a minor contribution by a Na^+-dependent system (e.g., system A, ASC and/or other unknown systems). Increased expression of system L transporters has been observed in various tumors [6], and, using DNA chips, we confirmed LAT1 in DLD-1 (data not shown).

It has been reported that the majority of [^{123}I]IMT transport in tumor cells involves the Na^+-independent system L, and that Na^+-dependent transport systems make a relatively minor contribution [5]. We recently examined the isoform selectivity of [^{125}I]IMT transport using two human L-type amino acid transporters (components of system L), LAT1 and LAT2, in *Xenopus laevis* oocytes coexpressing human LAT1 and human 4F2hc; [^{125}I]IMT transport was found to be LAT1 specific. LAT1 is expressed in various tumor tissues at higher levels than in normal tissues [5,20]. Lahoutte et al. [21] reported that system T also mediates [^{123}I]IMT transport into U266 human myeloma cells.

Amino acid transport systems are involved in [^{125}I]IMT uptake in the kidney. Our recent in vivo study confirmed that [^{125}I]IMT uptake into normal human renal proximal tubule epithelial cells was significantly inhibited by BCH in a Na^+-dependent manner, which suggests that [^{125}I]IMT was mainly reabsorbed via system B^0 in the apical membrane of the proximal tubules [9]. As shown in Fig. 2, [^{125}I]IMT uptake into the renal proximal tubule S1-distributed region (outer side of the kidney cortex) was significantly inhibited by BCH in a Na^+-dependent manner, thus suggesting reabsorption via amino acid transport system B^0 in the apical membrane of proximal tubules in vivo.

In the kidney, there was significant inhibition of [^{125}I]IMT uptake into S2 with PAH and PBC loading. Metabolically stable [^{125}I]IMT is derived from 3-iodo-L-tyrosine, based on reports that α-methylation confers metabolic stability to L-tyrosine [22,23] and also to 3-iodo-L-tyrosine. However, we recently proposed that α-methylated tyrosine analogues possess a higher affinity for accumulative renal organic anion secretion systems than non-α-methylated tyrosine analogues, because α-methylated tyrosine analogues such as [^{125}I]IMT and [^{18}F]FMT exhibit marked accumulation in the renal cortex [7,8]. Some studies have indicated that natural amino acid secretion and accumulation in proximal tubule cells is blocked by OAT inhibitors [24–26]. The cDNAs of six OAT isoforms have been cloned, and the molecular structures of those isoforms have been characterized [27]. There are two structural differences between natural L-tyrosine and [^{125}I]IMT: α-methylation and iodination of the 3 position of the L-tyrosine phenol group. These differences may be responsible for the greater affinity of ^{125}I]IMT for PBC-sensitive secretion. L-Tyrosine accumulation in kidney is moderate, in contrast to the high accumulation of IMT [28].

As described above, OAT inhibitors may have the potential to yield better tumor images. These compounds can presumably lead to prolonged and higher distribution of tracer to the tumor. Although we observed reduced accumulation in the renal cortex with PBC loading, this was insufficient. Improvements in dose and administration methods are anticipated. Other clinically available substrates of OATs (e.g., furosemide, ethacrynic acid and BBA) should also be tested for inhibition of kidney and tumor accumulation of [^{125}I]IMT.

5. Conclusions

We confirmed that [^{125}I]IMT transport is mediated by OATs in the proximal tubule S2-like region of the kidney, and by amino acid transport system L in DLD-1 cells. Reduced renal [^{125}I]IMT elimination by PBC loading led to higher tumor accumulation (target tissue) when compared to control conditions. We observed reduced accumulation in the renal cortex (nontarget tissue), but this was insufficient. Further study should result in improvements in dose and administration methods.

Acknowledgments

We wish to thank Natsumi Mibuka, Yuki Kitamura, Yuzou Taguchi, Miho Aoyama, Hironobu Sakai, Misako Nozaki, Yuko Fujisaku, Mariko Maruyama and Takayoshi Miyakawa of Ibaraki Prefectural University for their valuable technical assistance. This work was supported by Grants-in-Aid for Scientific Research (10770451, 14770498, 13557075, 15659283, 16659322 and 17390336) from the Ministry of Education, Science, Sports and Culture of Japan and the Japan Society for the Promotion of Science. Financial support was also provided by the Ibaraki Prefectural University Research Project (9808, 0118, 0220 and 0634) and Grants-in-Aid for the Encouragement of Young Scientists from Ibaraki Prefectural University of Health Sciences in 2001, 2002, 2004, 2005 and 2006.

References

[1] Biersack HJ, Coenen HH, Stöcklin G, Reichmann K, Bockisch A, Oehr P, et al. Imaging of brain tumors with L-3-[I-123]iodo-α-methyl tyrosine and SPECT. J Nucl Med 1989;30:110–2.

[2] Kuwert T, Woesler B, Morgenroth C, Lerch H, Schafers M, Palkovic S, et al. Diagnosis of recurrent glioma with SPECT and iodine-123-α-methyl tyrosine. J Nucl Med 1998;39:23–7.

[3] Jager PL, Franssen EJ, Kool W, Szabo BG, Hoekstra HJ, Groen HJ, et al. Feasibility of tumor imaging using L-3-[iodine-123]-iodo-alpha-methyl-tyrosine in extracranial tumors. J Nucl Med 1998;39: 1736–43.

[4] Langen K-J, Pauleit D, Coenen HH. 3-[^{123}I]Iodo-α-methyl-L-tyrosine: uptake mechanisms and clinical applications. Nucl Med Biol 2002;29: 625–31.

[5] Shikano N, Kanai Y, Kawai K, Ishikawa N, Endou H. Characterization of 3-[^{125}I]iodo-α-methyl-L-tyrosine transport via human L-type amino acid transporter 1. Nucl Med Biol 2003;30:31–7.

[6] Yanagida O, Kanai Y, Chairoungdua A, Kim DK, Segawa H, Nii T, et al. Human L-type amino acid transporter 1 (LAT1): characterization of function and expression in tumor cell lines. Biochim Biophys Acta 2001;1514:291–302.

[7] Inoue T, Koyama K, Oriuchi N, Alyafei S, Yuan Z, Suzuki H, et al. Detection of malignant tumors: whole-body PET with fluorine 18 alpha-methyl tyrosine versus FDG-preliminary study. Radiology 2001; 220:54–62.

[8] Shikano N, Kawai K, Flores II LG, Nishii R, Kubota N, Ishikaw N, et al. An artificial amino acid 4-iodo-L-*meta*-tyrosine: biodistribution and excretion via kidney. J Nucl Med 2003;44:625–31.

[9] Shikano N, Kawai K, Nakajima S, Nishii R, Flores II LG, Kubodera A, et al. Renal accumulation and excretion of radioiodinated 3-iodo-alpha-methyl-L-tyrosine. Ann Nucl Med 2004;18:263–70.

[10] Shikano N, Nakajima S, Kotani T, Itoh Y, Nishii R, Yoshimoto M, et al. Detection of maleate-induced Fanconi syndrome by decreasing accumulation of ^{125}I-3-iodo-alpha-methyl-L-tyrosine in the proximal tubule segment-1 region of renal cortex in mice: a trial of separate evaluation of reabsorption. Ann Nucl Med 2006;20:175–81.

[11] Shikano N, Kanai Y, Kawai K, Ishikawa N, Endou H. Transport of ^{99cm}Tc-MAG3 via rat renal organic anion transporter 1. J Nucl Med 2004;45:80–5.

[12] Christensen HN. Role of amino acid transport and counter-transport in nutrition and metabolism. Physiol Rev 1990;70:43–77.

[13] Palacin M, Estevenz R, Bertran E, Zorano A. Molecular biology of mammalian plasma membrane amino acid transports. Physiol Rev 1998;78:969-1054.

[14] Hirouchi Y, Naganuma H, Kawahara Y, Okada R, Kamiya A, Inui K, et al. Protective effect of *N*-acyl amino acids (NAAs) on cephaloridine (CER) nephrotoxicity in rabbits. Jpn J Pharmacol 1993;63:487–93.

[15] Sekine T, Cha SH, Hosoyamada M, Kanai Y, Watanabe N, Fukuda K, et al. Cloning, functional characterization and localization of a rat renal Na-dicarbrboxylate transporter. Am J Physiol 1998;275:F298-F305.

[16] Rosenberg LE, Blair A, Segal S. Transport of amino acids by slices of rat-kidney cortex. Biochim Biophys Acta 1961;54:479–88.

[17] McDonald TF, MacLeod DP. DNP-induced dissipation of ATP in anoxic ventricular muscle. J Physiol 1973;229:583–99.

[18] Langen K-J, Muhlensiepen H, Holschibach M, Hautzel H, Jansen P, Coenen HH. Transport mechanisms of 3-[^{123}I]iodo-α-methyl-L-tyrosine in a human glioma cell line: comparison with [^{3}H-methyl]-L-methionine. J Nucl Med 2000;41:1250–5.

[19] Kawai K, Fujibayashi Y, Saji H, Yonekura Y, Konishi J, Kubodera A, et al. A strategy for study of cerebral amino acid transport using iodine-123-labeled amino acid radiopharmaceutical: 3-iodo-alpha-methyl-L-tyrosine. J Nucl Med 1991;32:819–24.

[20] Shikano N, Kanai Y, Kawai K, Inatomi J, Kim DK, Ishikawa N, et al. Isoform selectivity of 3-^{125}I-iodo-alpha-methyl-L-tyrosine membrane transport in human L-type amino acid transporters. J Nucl Med 2003; 44:244–6.

[21] Lahoutte T, Caveliers V, Dierickx L, Vekeman M, Everaert H, Mertens J, et al. In vitro characterization of the influx of 3-[^{125}I]iodo-L-alpha-methyltyrosine and 2-[^{125}I]iodo-L-tyrosine into U266 human myeloma cells: evidence for system T transport. Nucl Med Biol 2001;28:129–34.

[22] Cooper JR, Bloom FE, Roth RH. Catecholamine. I. General aspects. The biochemical basis of neuropharmacology. 5th ed. New York: Oxford University Press; 1984. p. 203–58.

[23] Mimnaugh MN, Gearien JE. Adrenergic drugs. In: Foye WO, editor. Principles of medicinal chemistry. 3rd ed. Philadelphia: Lea & Febiger; 1989. p. 343–58.

[24] Williams WM, Huang KC. Structural specificity in the renal tubular transport of tyrosine. J Pharmacol Exp Ther 1981;219:69–74.

[25] Hang KC. Renal excretion of L-tyrosine and its derivatives. J Pharmacol Exp Ther 1961;134:257–65.

[26] Hang KC, Knoefel PK. Biochemorphology of renal tubular transport: halogenated amino acids and derivatives. J Pharmacol Exp Ther 1957; 121:443–8.

[27] Anzai N, Kanai Y, Endou H. Organic anion transporter family: current knowledge. J Pharmacol Sci 2006;100:411–26.

[28] Jager PL, Vaalburg W, Pruim J, de Vries EGE, Langen K-J, et al. Radiolabeled amino acids: basic aspects and clinical applications in oncology. J Nucl Med 2001;42:432–45.